Surface elevation change and mass balance of Icelandic ice caps derived from swath mode CryoSat-2 altimetry

L. Foresta, N. Gourmelen, F. Pálsson, P. Nienow, H. Björnsson, A. Shepherd

AGU PUBLICATIONS

Geophysical Research Letters

RESEARCH LETTER
10.1002/2016GL071485

Key Points:
- Icelandic ice cap elevation change is the result of complex interaction between climate, ice dynamics, and geothermal and magmatic processes
- Estimated rate of Icelandic mass loss between 2010 and 2015 is 5.8 ± 0.7 Gt a^{-1} contributing 0.016 ± 0.002 mm a^{-1} to sea level rise
- Swath processing improves on conventional POCA radar altimetry by providing elevation change with a twofold increase in spatial coverage

Supporting Information:
- Supporting Information S1

Correspondence to:
L. Foresta,
luca.foresta@ed.ac.uk

Citation:
Foresta, L., N. Gourmelen, F. Pálsson, P. Nienow, H. Björnsson, and A. Shepherd (2016), Surface elevation change and mass balance of Icelandic ice caps derived from swath mode CryoSat-2 altimetry, *Geophys. Res. Lett.*, *43*, 12,138–12,145, doi:10.1002/2016GL071485.

Received 5 OCT 2016
Accepted 14 NOV 2016
Accepted article online 16 NOV 2016
Published online 10 DEC 2016

Surface elevation change and mass balance of Icelandic ice caps derived from swath mode CryoSat-2 altimetry

L. Foresta[1], N. Gourmelen[1,2], F. Pálsson[3], P. Nienow[1], H. Björnsson[3], and A. Shepherd[4]

[1]School of GeoSciences, University of Edinburgh, Edinburgh, UK, [2]IPGS UMR 7516, Université de Strasbourg, CNRS, Strasbourg, France, [3]Institute of Earth Sciences, University of Iceland, Reykjavík, Iceland, [4]Centre for Polar Observation and Modelling, School of Earth and Environment, University of Leeds, Leeds, UK

Abstract We apply swath processing to CryoSat-2 interferometric mode data acquired over the Icelandic ice caps to generate maps of rates of surface elevation change at 0.5 km postings. This high-resolution mapping reveals complex surface elevation changes in the region, related to climate, ice dynamics, and subglacial geothermal and magmatic processes. We estimate rates of volume and mass change independently for the six major Icelandic ice caps, 90% of Iceland's permanent ice cover, for five glaciological years between October 2010 and September 2015. Annual mass balance is highly variable; during the 2014/2015 glaciological year, the Vatnajökull ice cap (~70% of the glaciated area) experienced positive mass balance for the first time since 1992/1993. Our results indicate that between glaciological years 2010/2011and 2014/2015 Icelandic ice caps have lost 5.8 ± 0.7 Gt a^{-1} on average, ~40% less than the preceding 15 years, contributing 0.016 ± 0.002 mm a^{-1} to sea level rise.

1. Introduction

It is estimated that glaciers and ice caps worldwide, including the periphery of the Greenland and Antarctic ice sheets, contribute about 47% of all land ice mass loss and 30% of current sea level rise [*Intergovernmental Panel on Climate Change*, 2013; *Gardner et al*., 2013]. Although satellite laser and radar altimetry observations have been crucial in estimating ice cap contributions to sea level change [*Bolch et al*., 2013; *Moholdt et al*., 2010a, 2010b; *Nuth et al*., 2010; *Rinne et al*., 2011a, 2011b; *Gardner et al*., 2011; *Moholdt et al*., 2012; *Nilsson et al*., 2015a; *McMillan et al*., 2014a], a comprehensive assessment is still lacking because of their complex topography, high slopes, and small size with respect to satellite ground track spacing (7.5 km and 40 km at 60°N for Icesat and Envisat, respectively) and footprint (2–10 km in diameter for Envisat). The European Space Agency CryoSat-2 (CS2) satellite [*Wingham et al*., 2006] carries a state-of-the-art radar altimeter for land ice applications. CS2 improves upon previous missions in three ways: (1) narrow intertrack spacing (4 km at 60°N) provides higher observation density, (2) synthetic aperture radar processing along track reduces the footprint size from ~1.65 × 1.65 km^2 (pulse limited) to ~1.65 × 0.305 km^2 (pulse-Doppler limited), and (3) the interferometer onboard CS2, in the so-called SARIn mode, allows the position of the surface reflection to be accurately located [*Wingham et al*., 2006]. Although these characteristics make standard CS2 SARIn elevations better suited to monitoring relatively small ice bodies characterized by complex and steep terrain [*McMillan et al*., 2014a; *Gray et al*., 2015], conventional point-of-closest-approach (POCA) altimetry tends to provide inhomogeneous spatial coverage due to the tendency of POCA toward sampling topographic highs (Figures S4 and S6 in the supporting information) [*Gray et al*., 2015].

Iceland is located at the boundary between polar and midlatitude atmospheric circulation cells and between the warm Irminger and cold East Greenland/East Iceland oceanic currents. As a consequence, Icelandic ice caps are very sensitive to climatic shifts [e.g., *Björnsson et al*., 1998, 2013; *Aðalgeirsdóttir et al*., 2005; *Flowers et al*., 2005] and are estimated to have the highest static mass balance sensitivities among glaciers and ice caps north of 60° [*de Woul and Hock*, 2005]. They also display highly complex and dynamic behavior unique to Iceland; about 60% of the current glaciated area lies over active volcanoes [*Björnsson and Pálsson*, 2008] and subglacial eruptions episodically trigger rapid ice loss albeit on short time scales (<1 year [*Björnsson et al*., 2013]). Furthermore, surge-type outlet glaciers are present in all Icelandic ice caps and cover 75% of Vatnajökull's surface [*Björnsson et al*., 2003]; surges in Iceland can cause significant mass transport to the ablation area and advance the terminus by up to 10 km during surge, with an opposite effect during multidecadal postsurge periods [*Björnsson et al*., 2003; *Björnsson and Pálsson*, 2008; *Gourmelen et al*., 2011]. Icelandic ice caps have been losing mass since the mid-1990s, in response to rising air temperatures caused by changes

in atmospheric and oceanic circulation around Iceland, possibly induced by a weakening of the North Atlantic subpolar gyre [*Björnsson et al.*, 2013 and references therein]. Vatnajökull, with a loss of 6.58 Gt a^{-1} between 1995 and 2010, is the main contributor to the overall regional mass loss, followed by Langjökull (1.31 Gt a^{-1} between 1997 and 2010) and Hofsjökull (1.24 Gt a^{-1} between 1995 and 2010) in the central highlands (Table 1) [*Björnsson et al.*, 2013]. Iceland as a whole has lost mass at a rate of ~11.0 ± 1.5 Gt a^{-1} in the period of 2003–2010 and contributed 0.03 ± 0.004 mm a^{-1} to sea level rise [e.g., *Björnsson et al.*, 1998, 2002, 2013; *Guðmundsson et al.*, 2011; *Jacob et al.*, 2012; *Gardner et al.*, 2013; *Pálsson et al.*, 2012; *Jóhannesson et al.*, 2013; *Hannesdóttir et al.*, 2015; *Magnússon et al.*, 2016; *Pope et al.*, 2016]. However, interannual variability is high, with rates of mass loss varying from 2 to 25 Gt a^{-1} between 1995 and 2009 [*Björnsson et al.*, 2013]. This reflects both variability in tephra deposition on the ice caps [e.g., *Möller et al.*, 2014] as well as their high sensitivity to temperature and precipitation [*Björnsson et al.*, 2013; *Aðalgeirsdóttir et al.*, 2006; *de Woul and Hock*, 2005].

Here we extend mass balance estimates of the Icelandic ice caps from 2010 to 2015, by exploiting CS2 as a swath altimeter. We estimate the annual rate of mass change of Iceland's six largest ice caps, Vatnajökull, Langjökull, Hofsjökull, Mýrdalsjökull, Drangajökull, and Eyjafjallajökull, corresponding to 90% of the island's permanent ice cover, and over 99% of its volume [*Björnsson and Pálsson*, 2008].

2. Methods

We measure time-dependent elevation over the ice caps by using swath processing of CS2 level 1b SARIn data (SwSARIn). In contrast to the conventional POCA method, SwSARIn exploits the full radar waveform to provide a dense swath of elevation measurements across the satellite ground track (beyond POCA) when signal and surface conditions are favorable (see the supporting information) [*Hawley et al.*, 2009; *Gray et al.*, 2013; *Christie et al.*, 2016; *Ignéczi et al.*, 2016]. As a reference, we also use elevations derived from the operational CS2 level 2 POCA product to assess ice cap elevation changes (see the supporting information), where POCA refers to the CS2 heights obtained via conventional retracking [*Wingham et al.*, 2006]. For both data sets, we use CS2 baseline C data which are available from July 2010 to present.

We compute rates of surface elevation change $\dot{h}$ from SwSARIn data by using a plane-fit algorithm [*McMillan et al.*, 2014b] over five glaciological years: 2010/2011 to 2014/2015 (Figure 1). We define one glaciological year as the period between 1 October in year n and 30 September in year $n+1$. The dense elevation field provided by SwSARIn processing allows gridding at 0.5 km posting. In each pixel, the time-dependent elevation is obtained by

$$z(x, y, t) = c_0 x + c_1 y + \dot{h} t + c_2 \quad (1)$$

where x, y, t are easting, northing, and time, respectively. The time-dependent coefficient retrieved from the model fit is the linear rate of surface elevation change, $\dot{h}$. The model is iteratively fitted to the data, excluding elevation differing from the model by more than 3 standard deviations, until no more outliers are detected. The pixel rate uncertainty $\varepsilon_{\dot{h}}$ is extracted from the covariance matrix of the model parameters (see Text S2 in the supporting information). Pixels are discarded whenever a set of quality thresholds are exceeded (see Text S4), and final coverages of the rates of surface elevation change maps are 80% (Vatnajökull), 75% (Langjökull), 87% (Hofsjökull), 69% (Mýrdalsjökull), 65% (Drangajökull), and 27% (Eyjafjallajökull), respectively. No smoothing is applied, in order to minimize the correlation between adjacent measurements that would otherwise impact on the analysis of spatial variability in $\dot{h}$, and is permitted by the high observation density provided by SwSARIn.

We interpolate gaps in the maps of surface elevation change rates (Figure 1) by using hypsometric averaging [e.g., *Moholdt et al.*, 2010a; *Nilsson et al.*, 2015a] as a form of regionalization method and calculate ice cap volume changes from the gap filled maps (we do not use the method to extrapolate beyond the locus of the SWSARin measurements). We apply the regionalization independently for all of the ice caps except for Eyjafjallajökull which has relatively few measurements and is therefore processed together with the neighboring Mýrdalsjökull. The resulting $\dot{h}$ map is divided into 50 m elevation bands by using an external digital elevation model (DEM) from the National Land Survey of Iceland (Landmælingar Íslands, www.lmi.is), and the volume change $\dot{V}_k$ of each band k is calculated as the product of the mean $\dot{h}_k$ and the surface area A_k.

Table 1. Mass Balance of Icelandic Ice Caps

	A (km^2)	V (km^3)	$\dot{M}$ (Gt a^{-1}) (period)	$\dot{M}$ (Gt a^{-1})	$\dot{M}$ (m_{we} a^{-1})
Vatnajökull	8,100	3,100	−6.58[a] (1995–2010)	−3.68* ± 0.61	−0.52* ± 0.09
	900	190	−1.31[a] (1997–2010)		
Langjökull				−0.70 ± 0.20	−0.81 ± 0.23
			−1.20[d] (1999–2007)		
Hofsjökull	890	200	−1.24[a] (1995–2010)	−0.45 ± 0.10	−0.66 ± 0.15
			−0.92[b] (2004–2008)		
Mýrdalsjökull + Eyafjallajökull	590 + 80	140		−0.21 ± 0.16	−0.39 ± 0.29
			−0.06[b] (2004–2010)		
Drangajökull	160	24	−0.07[c] (2005–2011)	−0.05 ± 0.07	−0.28 ± 0.40
			−0.05[b] (1990–2011)		
Iceland	~11,000	~3,600	−[9–11] ± [1–3][a,e,f,g] (~1995–2010)	−5.83 ± 0.74	−0.59 ± 0.07

Estimates from SwSARIn data for five glaciological years between October 2010 and September 2015, as well as from the current literature (with respect to the specified time period). Mass change $\dot{M}$ is given in Gt a^{-1} as well as m_{we} a^{-1} (specific mass balance). Ice cap areas and volumes after *Björnsson and Pálsson* [2008].
[a]*Björnsson et al.* [2013].
[b]*Jóhannesson et al.* [2013].
[c]*Magnússon et al.* [2016].
[d]*Pálsson et al.* [2012].
[e]*Gardner et al.* [2013].
[f]*Jacob et al.* [2012].
[g]*Nilsson et al.* [2015a].
*Mass balance of Vatnajökull between October 2010 and September 2014 is −4.93 ± 0.80 Gt a^{-1} (−0.69 ± 0.11 m_{we} a^{-1}).

The DEM spatial resolution is downscaled to the $\dot{h}$ grid resolution so that pixel elevations and elevation bands areas are representative of the pixel size. Volume change estimates for all bands are added together and then converted to a mass balance rate $\dot{M}$ by using the density of glacial ice. Although this simplification ignores potential variations in snow/firn density (e.g., with elevation and thus melt), it is commonly used when deriving mass change and sea level contribution from ice caps [e.g., *Magnússon et al.*, 2016; *Nilsson et al.*, 2015a; *Nuth et al.*, 2010; *Moholdt et al.*, 2010b; *Björnsson et al.*, 2013]. For comparison, we also provide a mass balance estimate assuming a dual density scenario [e.g., *Gardner et al.*, 2011; *Moholdt et al.*, 2010a] to account for density differences between the ablation and accumulation area. We propagate rate errors $\varepsilon_{\dot{h}}$ of the individual pixels to estimate uncertainties for $\dot{V}$ and $\dot{M}$ (see the supporting information).

3. Results

SwSARIn provides a step-change in surface coverage (Figure 1), generating ~10 million elevation measurements over Vatnajökull between October 2010 and September 2015 and allowing the retrieval of rates of surface elevation change over 80% of the ice cap area (Figure S5). In comparison, ICESat acquired 851 elevation measurements over all Icelandic ice caps between 2003 and 2009 [*Nilsson et al.*, 2015a]. With the conventional POCA approach, CS2 delivers ~60,000 observations over Vatnajökull (October 2010 to September 2015) and provides rates of surface elevation change over 40% of the ice cap area, preferentially along topographic highs (see Text S3 and Figure S4). Over the Langjökull ice cap, the particular hypsometry accentuates the concentration of elevations over the ice divide (inset in Figures 1; Figure S6). There is almost no POCA observation close to the marginal areas of the northern dome (Figure S8, middle) and only ~10 observation per km^2 over the southern dome (Figure S8, right), which is insufficient to estimate robust rates of surface elevation change. In turn, limited sampling at the margins where most of the thinning is occurring impacts on the representativity of the POCA rates of volume and mass change (see Text S3).

The time series of surface elevation change over the Vatnajökull ice cap (Figure 2) shows a clear seasonal pattern with an increase in surface elevation during the accumulation period followed by a rapid decrease during the melt season, with amplitudes of about 3 m similar to observations over other Arctic ice caps [*Gray et al.*, 2015]. Additionally, the elevation time series show an absence of sharp jumps in elevation that would otherwise be indicative of a sudden and unusual change in scattering horizon and would introduce a bias in the estimated rates of surface elevation change [*Nilsson et al.*, 2015b; *McMillan et al.*, 2016].

The data reveal a clear pattern of thinning, with rates of up to 10 m a^{-1} over most of the marginal areas of the ice caps, while change in the ice cap interior is more heterogeneous with both thinning and thickening

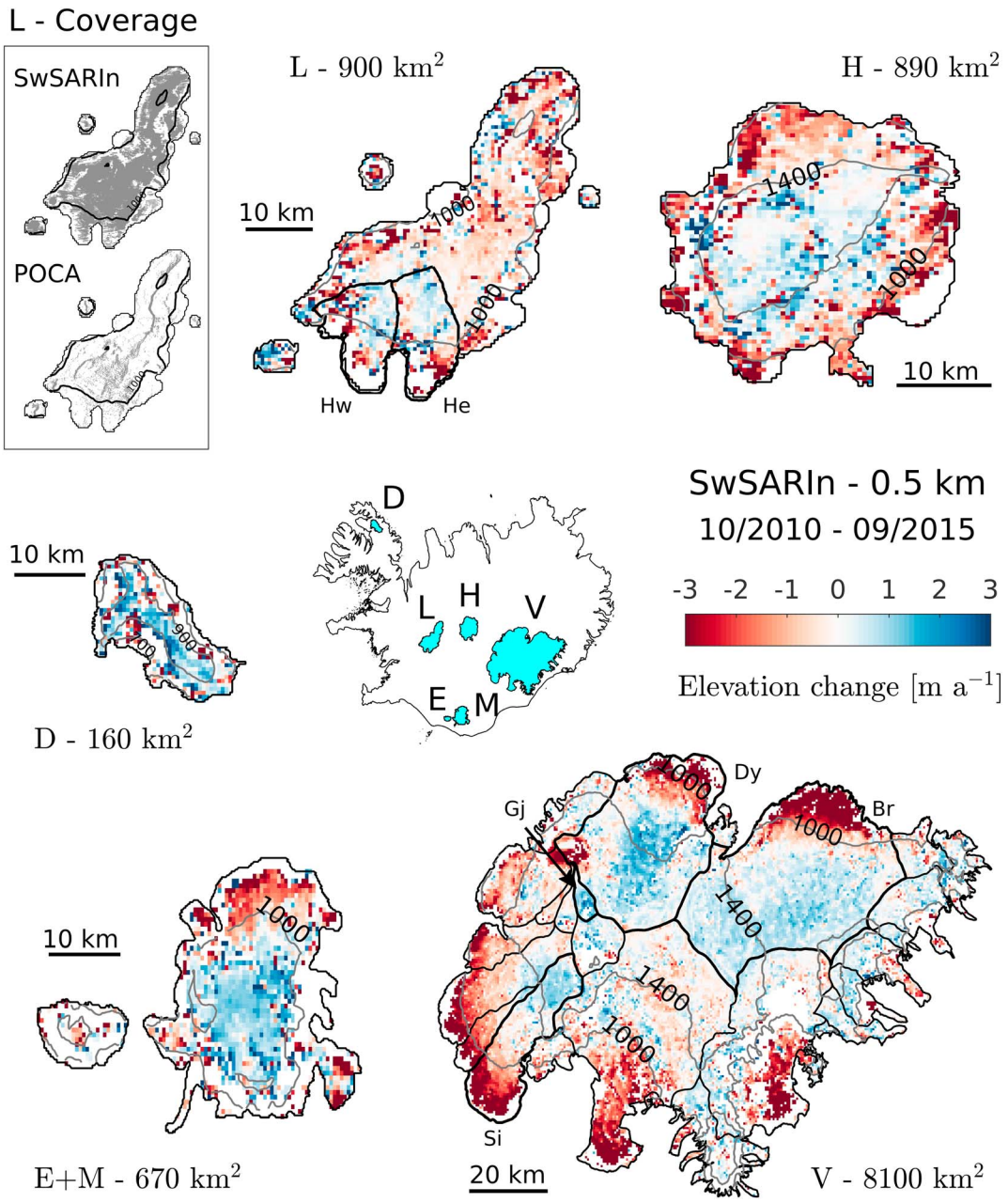

Figure 1. Rates of surface elevation change maps of Icelandic ice caps between 2010 and 2015 at 0.5 km posting based on SwSARIn heights as well as location of the ice caps in Iceland. V (Vatnajökull), L (Langjökull), H (Hofsjökull), M (Mýrdalsjökull), D (Drangajökull), and E (Eyjafjallajökull). Basin outlines are shown in thin black lines. Selected basins over Vatnajökull and Langjökull are Brúarjökull (Br), Síðujökull (Si), Dyngjujökull (Dy), Gjálp (Gj), Hagafellsjökull West (Hw), and Hagafellsjökull East (He) (thick black outlines). Ice cap areas after *Björnsson and Pálsson* [2008]. Contour elevations are shown in grey. The inset shows the location of individual elevation measurements by using SwSARIn and POCA approaches over Langjökull.

observed (Figure 1). This variability in the interior is particularly apparent over Vatnajökull, where several basins—e.g., Brúarjökull (Br), Síðujökull (Si), and Dyngjujökull (Dy)—are thickening at high elevation, while Skeiðarárjökull (east of Si) is thinning over almost its entire area. Thinning of Langjökull in the central highlands is widespread on the ice cap's surface up to, and including, the ice divide, while neighboring Hofsjökull shows thickening over the center and thinning over the margins. In the south of Iceland, relatively high rates of thickening (up to 3 m a^{-1}) are widespread over Mýrdalsjökull's central plateau. Thinning is visible particularly on its northern slopes which lie at low elevations as well as on the steeper southern margins.

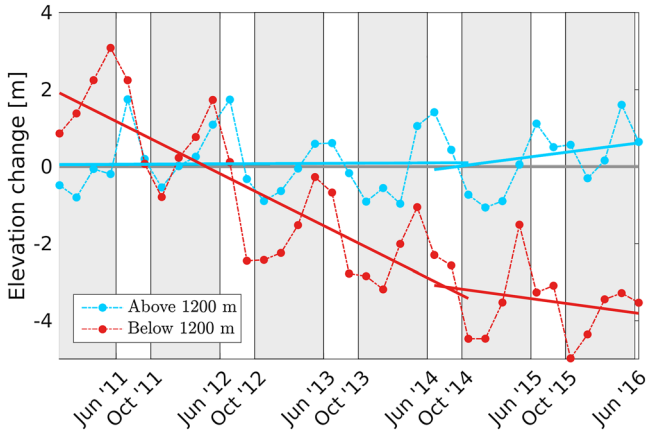

Figure 2. Vatnajökull elevation time series (60 days step) produced from SwSARIn elevations above and below 1200 m, used as an approximate ice cap wide ELA. The dark grey bands highlight the accumulation period between October and May; the nonshaded area corresponds to the ablation period between June and September. The two trends show mean rates of elevation change between 2010–2014 and between 2014–2016.

In the same region and despite being exposed to a similar climate, Eyjafjallajökull shows signs of thinning at its summit; however, coverage here is limited due to the small area (~80 km^2) and steep hypsometry (~700–1560 m). Drangajökull (northwest) mostly displays a thickening pattern in the comparatively large accumulation area.

We use the CS2-derived rates of surface elevation change to compute mean annual rates of ice cap volume and mass change over five glaciological years from October 2010 to September 2015 (Table 1). During this time, we estimate that the Vatnajökull ice cap (~70% of Iceland's glaciated area) is losing mass at a rate of $3.68 \pm 0.61\,Gt\,a^{-1}$ ($-0.52 \pm 0.09\,m_{we}\,a^{-1}$) and is the main contributor (63%) to mass loss in Iceland, followed by Langjökull (12%) and Hofsjökull (8%) in central Iceland (Table 1). Langjökull is the fastest changing ice cap with $-0.81 \pm 0.23\,m_{we}\,a^{-1}$ specific mass balance, followed by Hofsjökull and Vatnajökull with $-0.66 \pm 0.15\,m_{we}\,a^{-1}$ and $-0.52 \pm 0.09\,m_{we}\,a^{-1}$, respectively (Table 1). A combined estimate is generated for Mýrdalsjökull and Eyjafjallajökull (3.6% of loss) since data coverage over the latter is limited and the two ice caps are exposed to similar climatic conditions. To the northwest, Drangajökull appears to be close to balance ($-0.05 \pm 0.07\,Gt\,a^{-1}$; $-0.28 \pm 0.40\,m_{we}\,a^{-1}$); the uncertainty is comparatively large due to the small aerial extent and steep hypsometry of the ice cap (Table 1). Summing contributions from the six ice caps analyzed in this study, and rescaling for the remaining 10% glacierized area not included in our survey, we estimate Iceland lost ice at a rate of $5.83 \pm 0.74\,Gt\,a^{-1}$ ($-0.59 \pm 0.07\,m_{we}\,a^{-1}$) between October 2010 and September 2015, corresponding to $0.016 \pm 0.002\,mm\,a^{-1}$ eustatic sea level change. Assuming a dual-density scenario in the ablation and accumulation areas with $\rho_{abl} = 900\,kg\,m^{-3}$ and $\rho_{acc} = 650\,kg\,m^{-3}$, the mass loss and contribution to sea level change estimates are higher by just 4%, within the uncertainty of the single-density case. During the glaciological year 2014/2015, the Vatnajökull ice cap had positive mass balance (Figure 2), an unprecedented observation in the last two decades [*Björnsson et al.*, 2013] and due to anomalously high winter precipitation. This anomaly is reflected in the time series of surface elevation change where the trends in both the ablation and accumulation areas change after October 2014 (Figure 2). In the four glaciological years before 2014/2015, we find that Vatnajökull's rate of mass loss was $4.93 \pm 0.80\,Gt\,a^{-1}$ ($-0.69 \pm 0.11\,m_{we}\,a^{-1}$) or ~34% larger than the period of 2010/2011 to 2014/2015.

We compared our geodetic estimates for the Langjökull ice cap and the Brúarjökull basin of the Vatnajökull ice cap against in situ field-derived mass balance observations from ongoing surveys [e.g., *Björnsson et al.*, 1998, 2002, 2013; *Pálsson et al.*, 2012; *Jóhannesson et al.*, 2013]. We restricted the data sets to the same time period, four glaciological years from October 2010 to September 2014. The geodetic estimate for Langjökull, $-0.76 \pm 0.25\,Gt\,a^{-1}$ ($-0.92 \pm 0.30\,m_{we}\,a^{-1}$), is 38% less negative than that from the in situ data, $-1.05 \pm 0.36\,Gt\,a^{-1}$ ($-1.28 \pm 0.30\,m_{we}\,a^{-1}$), but the two values agree within uncertainties. Over the Brúarjökull basin the agreement is good, $-0.51 \pm 0.09\,Gt\,a^{-1}$ ($-0.37 \pm 0.07\,m_{we}\,a^{-1}$) compared to $-0.49 \pm 0.22\,Gt\,a^{-1}$ ($-0.35 \pm 0.30\,m_{we}\,a^{-1}$) for the geodetic and in situ values, respectively. Using a dual-density scenario, Langjökull's and Brúarjökull's geodetic mass balance estimates change by +17% and −18%, respectively.

4. Discussion

The heterogeneity of the rates of surface elevation change can be linked to the heterogeneity of ice cap hypsometry as well as their exposure to local climatic conditions, active volcanoes, and glacier surge events.

Individual basins of the Vatnajökull ice cap display distinct behaviors, either thinning across their entire length or experiencing thickening at high elevation. Three basins, namely, Brúarjökull, Síðujökull, and Dyngjujökull (Figure 1), show large areas of thickening at higher elevation, as they are currently in a post-surge stage, responding to surges that occurred in 1963, 1995, and 1999, respectively [*Björnsson et al*., 2003; *Fischer et al*., 2003]. Thickening in the Gjálp area (Figure 1), by an average of 0.7 m a^{-1}, is related to a combination of snow drift and ice inflow into the depression created by the 1996 subglacial volcanic eruption; these uplift rates are down from 40 m a^{-1} as measured in the year following the eruption [*Guðmundsson et al*., 2002]. North of Gjálp, over the Bárðarbunga central volcano caldera ice surface, the strong subsidence pattern is the surface response to the Bárðarbunga eruption that occurred between August 2014 and March 2015 [*Sigmundsson et al*., 2014; *Guðmundsson et al*., 2016]. This event deflated a magma chamber below the ~700 m thick ice; little or no ice was melted, but the caldera bedrock floor lowered by tens of meters and the ice above lowered similarly forming a cauldron like surface subsidence with a volume of ~1.9 km^3 [*Sigmundsson et al*., 2014; *Guðmundsson et al*., 2016]. The impact of this area on the ice cap wide rate of volume change is 0.05 $km^3 a^{-1}$ (~1% of Vatnajökull's total volume change). In the central highlands, and despite their close proximity and similar climatic conditions, the pattern of rates of surface elevation change of the Langjökull and Hofsjökull ice caps differs considerably, most likely due to their differing hypsometry. Despite having similar area and volume (~900 km^2 and ~200 km^3), Langjökull has a lower elevation range (430–1440 m above sea level (asl)) than Hofsjökull (620–1790 m asl) [*Björnsson and Pálsson*, 2008; *Guðmundsson et al*., 2009], and a large portion of the surface of Langjökull therefore lies close to the current equilibrium line altitude (ELA) [*Pálsson et al*., 2012]. Thickening is visible in the accumulation area of the West and East Hagafellsjökull basins of the Langjökull ice cap (Figure 1) and is a dynamic response to the 1980 and 1999 surge events, respectively [*Björnsson et al*., 2003]. The central part of the Mýrdalsjökull ice cap is thickening at rates of about 1–3 m a^{-1}, although the surface elevation of the plateau has not changed compared to 1999. The thickening is most likely induced by the extreme precipitation in winter 2015, which deposited 10-15 m of snow of snow on the ice cap. Over Eyjafjallajökull's summit, the surface is thinning as ice flows into the crater created by the Eyjafjallajökull eruption in 2010 [*Oddsson et al*., 2016]. Over Drangajökull (northwest), despite the relatively small size of the ice cap as well as the steep elevation range, SwSARIn data capture the thinning pattern across the ablation area. This allows us to generate a robust estimate of mass balance, a result that cannot be achieved with conventional POCA processing (see Text S3 and Tables S1 and S2).

Geodetic mass balance derived from repeat altimetry is dependent on the regionalization method chosen to derive volume change from the rates of surface elevation change [e.g., *Nilsson et al*., 2015a]. The high density of measurements provided by SwSARIn allows us to regionalize at the ice cap scale and in some cases at the basin scale (e.g., Brúarjökull), better accounting for local differences, in contrast to data sets with a lower density of observations which require mean hypsometric related rates of surface elevation change to be averaged at the scale of Iceland as a whole [*Nilsson et al*., 2015a]. Thus, the hypsometric averaging method applied at the basin scale shows good agreement with the in situ estimate for one of Vatnajökull's largest basins: Brúarjökull. Comparing the SWSARIn and in situ mass balance estimates over the Langjökull ice cap instead shows a difference between the two approaches. Current interdrainage basin variability in rates of surface elevation change is relatively large in Iceland and is related to dynamic adjustment after glacier surges and subglacial eruptions as well as contrasting climatic conditions, e.g., due to inland precipitation shadow, hypsometry, or distance from the south coast (the North-Atlantic low path). For example, the south-eastern basins of Vatnajökull (e.g., as in *Aðalgeirsdóttir et al*. [2006]) reach low elevations at their termini, are exposed to high precipitation, and have infrequent surges [*Björnsson et al*., 2003]. In contrast, basins in the northwest are more affected by surges and their termini are above 700 m elevation. Applying a hypsometric model at the ice cap scale would clearly not capture this complexity. SwSARIn provides a step change from previous altimetry-based techniques in mapping the complexity of ice caps' response to internal and external forcing as it enables the independent monitoring of individual ice caps. Additionally, the method can be used to derive mass balance estimates at the individual basin scale (e.g Brúarjökull).

5. Conclusions

CryoSat-2 swath radar interferometric altimetry (SwSARIn) increases the density of surface elevation measurements over Icelandic ice caps by 2 and 5 orders of magnitude with respect to the conventional

point-of-closest-approach (POCA) method applied to the CryoSat-2 and ICESat missions, respectively. Compared to POCA measurements, which tend to concentrate on topographic highs, SwSARIn samples a wider range of elevations which helps generate more reliable estimates of mass balance, particularly for Icelandic ice caps with complex hypsometry. Swath altimetry allows high-resolution mapping of surface elevation and its temporal change revealing complex spatiotemporal patterns of surface elevation change related to climatic, dynamic, and subglacial processes in Iceland. We estimate that Icelandic ice caps have lost a total of $5.8 \pm 0.7\,\mathrm{Gt\,a^{-1}}$ ($-0.6 \pm 0.1\,\mathrm{m_{we}\,a^{-1}}$) between October 2010 and September 2015, equivalent to $0.016 \pm 0.002\,\mathrm{mm\,a^{-1}}$ eustatic sea level change. This estimate suggests that over this 5 year period, the mass balance was 40% less negative than the preceding 15 years, a fact which partly reflects the anomalous positive balance year across Vatnajökull in 2014/2015. Our observations also demonstrate the capability of SwSARIn elevations to image glaciological processes occurring at the subcatchment scale, and to infer global, time-dependent, mass balance over region of complex hypsometry such as ice caps and ice sheet margins.

Acknowledgments

This work was performed under the European Space Agency (ESA) Support to Science Elements CryoSat+ CryoTop contract 4000107394/12/I-NB, CS+ Mountain Glaciers contract 4000114224/15/I-SBo to N.G. and A.S., and ESA CryoSAT-LI contract 4000109790/13/NL/CT/ab to N.G., P.N., and A.S. L.F. acknowledges a Young Scientist Training grant from the ESA Dragon3 program. The authors wish to thank ESA for providing open access to CryoSat-2 data and the National Land Survey of Iceland (Landmælingar Íslands, www.lmi.is) for providing open access to a digital elevation model of Iceland. The authors are grateful to the Editor, Julienne Stroeve, and to two anonymous reviewers, whose comments have significantly improved the manuscript.

References

Aðalgeirsdóttir, G., G. H. Guðmundsson, and H. Björnsson (2005), The volume sensitivity of Vatnajökull Ice Cap, Iceland, to perturbations in equilibrium line altitude, *J. Geophys. Res.*, *110*, F04001, doi:10.1029/2005JF000289.

Aðalgeirsdóttir, G., T. Jóhannesson, H. Björnsson, F. Pálsson, and O. Sigurðsson (2006), Response of Hofsjökull and southern Vatnajökull, Iceland, to climate change, *J. Geophys. Res.*, *111*, F03001, doi:10.1029/2005JF000388.

Björnsson, H., and F. Pálsson (2008), Icelandic glaciers, *Jökull*, *58*, 365–386.

Björnsson, H., F. Pálsson, M. T. Guðmundsson, and H. H. Haraldsson (1998), Mass balance of western and northern Vatnajökull, Iceland, 1991–1995, *Jökull*, *45*, 35–38.

Björnsson, H., F. Pálsson, and H. H. Haraldsson (2002), Mass balance of Vatnajökull (1991–2001) and Langjökull (1996–2001), Iceland, *Jökull*, *51*, 75–78.

Björnsson, H., F. Pálsson, O. Sigurðsson, and G. E. Flowers (2003), Surges of glaciers in Iceland, *Ann. Glaciol.*, *36*, 82–90.

Björnsson, H., F. Pálsson, S. Gudmundsson, E. Magnússon, G. Aðalgeirsdóttir, T. Jóhannesson, E. Berthier, O. Sigurdsson, and T. Thorsteinsson (2013), Contribution of Icelandic ice caps to sea level rise: Trends and variability since the Little Ice Age, *Geophys. Res. Lett.*, *40*, 1546–1550, doi:10.1002/grl.50278.

Bolch, T., L. S. Sørensen, S. B. Simonssen, N. Mölg, H. Machguth, P. Rastner, and F. Paul (2013), Mass loss of Greenland's glaciers and ice caps 2003–2008 revealed from ICESat laser altimetry data, *Geophys. Res. Lett.*, *40*, 875–881, doi:10.1002/grl.50270.

Christie, F. D. W., R. G. Bingham, N. Gourmelen, S. F. B. Tett, and A. Muto (2016), Four-decade record of pervasive grounding line retreat along the Bellingshausen margin of West Antarctica, *Geophys. Res. Lett.*, *43*, 5741–5749, doi:10.1002/2016GL068972.

de Woul, M., and R. Hock (2005), Static mass-balance sensitivity of Arctic glaciers and ice caps using a degree-day approach, *Ann. Glaciol.*, *1*, 217–224.

Fischer, A., H. Rott, and H. Björnsson (2003), Observation of recent surges of Vatnajökull, Iceland, by means of ERS SAR interferometry, *Ann. Glaciol.*, *37*, 69–76.

Flowers, G. E., S. J. Marshall, H. Björnsson, and G. K. C. Clarke (2005), Sensitivity of Vatnajökull ice cap hydrology and dynamics to climate warming over the next 2 centuries, *J. Geophys. Res.*, *110*, F02011, doi:10.1029/2004JF000200.

Gardner, A. S., G. Moholdt, B. Wouters, G. J. Wolken, D. O. Burgess, M. J. Sharp, J. G. Cogley, C. Braun, and C. Labine (2011), Sharply increased mass loss from glaciers and ice caps in the Canadian Arctic Archipelago, *Nature*, *473*, 357–360, doi:10.1038/nature10089.

Gardner, A. S., et al. (2013), A reconciled estimate of glacier contributions to sea level rise: 2003 to 2009, *Science*, *340*, 852–857, doi:10.1126/science.1234532.

Gourmelen, N., S. W. Kim, A. Shepherd, J. W. Park, A. Sundal, H. Björnsson, and F. Pálsson (2011), Ice velocity determined using conventional and multiple-aperture InSAR, *Earth Planet. Sci. Lett.*, *307*(1–2), 156–160, doi:10.1016/j.epsl.2011.04.026.

Gray, L., D. Burgess, L. Copland, R. Cullen, N. Galin, R. Hawley, and V. Helm (2013), Interferometric swath processing of Cryosat data for glacial ice topography, *Cryosphere*, *7*, 1857–1867, doi:10.5194/tc-7-1857-2013.

Gray, L., D. Burgess, L. Copland, M. N. Demuth, T. Dunse, K. Langley, and T. V. Schuler (2015), CryoSat-2 delivers monthly and inter-annual surface elevation change for Arctic ice caps, *Cryosphere*, *9*, 1895–1913, doi:10.5194/tc-9-1895-2015.

Guðmundsson, M. T., et al. (2016), Gradual caldera collapse at Bárðarbunga volcano, Iceland, regulated by lateral magma outflow, *Science*, *353*(6296), aaf8988, doi:10.1126/science.aaf8988.

Guðmundsson, S., M. T. Guðmundsson, H. Björnsson, F. Sigmundsson, H. Rott, and J. M. Carstensen (2002), Three-dimensional glacier surface motion maps at the Gjálp eruption site, Iceland, inferred from combining InSAR and other ice-displacement data, *Ann. Glaciol.*, *47*, 315–322.

Guðmundsson, S., H. Björnsson, T. Jóhannesson, G. Aðalgeirsdóttir, F. Pálsson, and O. Sigurðsson (2009), Similarities and differences in the response to climate warming of two ice caps in Iceland, *Hydrol. Res.*, *40*, 495–502.

Guðmundsson, S., H. Björnsson, E. Magnússon, E. Berthier, F. Pálsson, M. T. Guðmundsson, Þ. Högnadóttir, and J. Dall (2011), Response of Eyjafjallajökull, Torfajökull and Tindfjallajökull ice caps in Iceland to regional warming, deduced by remote sensing, *Polar Res.*, *30*, 7282, doi:10.3402/polar.v30i0.7282.

Hannesdóttir, H., H. Björnsson, F. Pálsson, G. Aðalgeirsdóttir, and S. Guðmundsson (2015), Changes in the southeast Vatnajökull ice cap, Iceland, between ~1890 and 2010, *Cryosphere*, *9*, 565–585, doi:10.5194/tc-9-565-2015.

Hawley, R. L., A. Shepherd, R. Cullen, V. Helm, and D. J. Wingham (2009), Ice-sheet elevations from across-track processing of airborne interferometric radar altimetry, *Geophys. Res. Lett.*, *36*, L22501, doi:10.1029/2009GL040416.

Ignéczi, Á., A. J. Sole, S. J. Livingstone, A. A. Leeson, X. Fettweis, N. Selmes, N. Gourmelen, and K. Briggs (2016), Northeast sector of the Greenland Ice Sheet to undergo the greatest inland expansion of supraglacial lakes during the 21st century, *Geophys. Res. Lett.*, *43*, 9729–9738, doi:10.1002/2016GL070338.

Intergovernmental Panel on Climate Change (2013), *Climate Change 2013—The Physical Science Basis. Contribution of Working Group I to the Fifth Assessment Report of the IPCC*, pp. 1–996, Cambridge Univ. Press, Cambridge, U. K., and New York.

Jacob, T., J. Wahr, W. T. Pfeffer, and S. Swenson (2012), Recent contributions of glaciers and ice caps to sea level rise, *Nature*, *482*, 514–518, doi:10.1038/nature10847.

Jóhannesson, T., H. Björnsson, E. Magnússon, S. Guðmundsson, F. Pálsson, O. Sigurðsson, T. Thorsteinsson, and E. Berthier (2013), Ice-volume changes, bias estimation of mass-balance measurements and changes in subglacial lakes derived by lidar mapping of the surface of Icelandic glaciers, *Ann. Glaciol.*, *54*, 63–74, doi:10.3189/2013AoG63A422.

Magnússon, E., J. Muñoz-Cobo Belart, F. Pálsson, H. Ágústsson, and P. Crochet (2016), Geodetic mass balance record with rigorous uncertainty estimates deduced from aerial photographs and lidar data—Case study from Drangajökull ice cap, NW Iceland, *Cryosphere*, *10*, 159–177, doi:10.5194/tc-10-159-2016.

McMillan, M., et al. (2014a), Rapid dynamic activation of a marine-based Arctic ice cap, *Geophys. Res. Lett.*, *41*, 8902–8909, doi:10.1002/2014GL062255.

McMillan, M., A. Shepherd, A. Sundal, K. Briggs, A. Muir, A. Ridout, A. Hogg, and D. Wingham (2014b), Increased ice losses from Antarctica detected by CryoSat-2, *Geophys. Res. Lett.*, *41*, 3899–3905, doi:10.1002/2014GL060111.

McMillan, M., et al. (2016), A high-resolution record of Greenland mass balance, *Geophys. Res. Lett.*, *43*, 7002–7010, doi:10.1002/2016GL069666.

Moholdt, G., C. Nuth, J. O. Hagen, and J. Kohler (2010a), Recent elevation changes of Svalbard glaciers derived from ICESat laser altimetry, *Remote Sens. Environ.*, *114*, 2756–2767.

Moholdt, G., J. O. Hagen, T. Eiken, and T. V. Schuler (2010b), Geometric changes and mass balance of the Austfonna ice cap, Svalbard, *Cryosphere*, *4*, 21–34.

Moholdt, G., B. Wouters, and A. S. Gardner (2012), Recent mass changes of glaciers in the Russian High Arctic, *Geophys. Res. Lett.*, *39*, L10502, doi:10.1029/2012GL051466.

Möller, R., M. Möller, H. Björnsson, S. Guðmundsson, F. Pálsson, B. Oddsson, P. A. Kukla, and C. Schneider (2014), MODIS-derived albedo changes of Vatnajökull (Iceland) due to tephra deposition from the 2004 Grímsvötn eruption, *Int. J. Appl. Earth Observ. Geoinf.*, *26*, 256–269.

Nilsson, J., L. S. Sorensen, V. R. Barletta, and R. Forsberg (2015a), Mass change of Arctic ice caps and glaciers: Implications of regionalizing elevation changes, *Cryosphere*, *7*, 5889–5920.

Nilsson, J., et al. (2015b), Greenland 2012 melt event effects on CryoSat-2 radar altimetry, *Geophys. Res. Lett.*, *42*, 3919–3926, doi:10.1002/2015GL063296.

Nuth, C., G. Moholdt, J. Kohler, J. O. Hagen, and A. Kääb (2010), Svalbard glacier elevation changes and contribution to sea level rise, *J. Geophys. Res.*, *115*, F01008, doi:10.1029/2008JF001223.

Oddsson, B., M. T. Gudmundsson, B. R. Edwards, T. Thordarson, E. Magnússon, and G. Sigurdsson (2016), Subglacial lava propagation, ice melting and heat transfer during emplacement of an intermediate lava flow in the 2010 Eyjafjallajökull eruption, *Bull. Volcanol.*, *78*, doi:10.1007/s00445-016-1041-4.

Pálsson, F., S. Guðmundsson, H. Björnsson, E. Berthier, E. Magnússon, and H. H. Haraldsson (2012), Mass and volume changes of Langjokull ice cap, Iceland, similar to 1890 to 2009, deduced from old maps, satellite images and in situ mass balance measurements, *Jökull*, *62*, 81–96.

Pope, A., I. C. Willis, F. Pálsson, N. S. Arnold, W. G. Rees, H. Björnsson, and L. Grey (2016), Elevation change, mass balance, dynamics and surging of Langjökull, Iceland from 1997 to 2007, *J. Glaciol.*, *62*(233), 497–511, doi:10.1017/jog.2016.55.

Rinne, E. J., A. Shepherd, S. Palmer, M. R. van den Broeke, A. Muir, J. Ettema, and D. Wingham (2011b), On the recent elevation changes at the Flade Isblink Ice Cap, northern Greenland, *J. Geophys. Res.*, *116*, F03024, doi:10.1029/2011JF001972.

Rinne, E., A. Shepherd, A. Muir, and D. Wingham (2011a), A comparison of recent elevation change estimates of the Devon Ice Cap as measured by the ICESat and EnviSAT satellite altimeters, *IEEE Trans. Geosci. Remote Sens.*, *49*, 1902–1910.

Sigmundsson, F., et al. (2014), Segmented lateral dyke growth in a rifting event at Bárðarbunga volcanic system, Iceland, *Nature*, *517*, 193–195.

Wingham, D. J., et al. (2006), CryoSat: A mission to determine the fluctuations in Earth's land and marine ice field, *Adv. Space Res.*, *37*, 841–871.